Turkish Journal of Water Science & Management
ISSN: 2536 474X / e-ISSN: 2564-7334

Volume: 5 Issue: 1 Year: 2021

Research Article

Hydrodynamic Modelling Using HİDROTÜRK Model

HİDROTÜRK Modeli Kullanılarak Hidrodinamik Modelleme

Lale Balas[1*], Kağan Cebe[2]
[1]*Gazi University, Sea and Aquatic Sciences Application and Research Center, Engineering Faculty, Civil Engineering Department, Ankara, Turkey*
lalebal@gazi.edu.tr (https://orcid.org/0000-0003-1916-1237)
[2]*Nevşehir Hacı Bektaş Veli University, Engineering-Architectural Faculty, Civil Engineering Department Nevşehir,Turkey*
kcebe@nevsehir.edu.tr (https://orcid.org/0000-0003-1288-1362)
Received Date: 12.05.2020, Accepted Date: 01.12.2020

Abstract

In this manuscript, the hydrodynamic sub-model components of HİDROTÜRK, the first national hydrological, hydrodynamic, hydrogeological, water quality, and ecological model developed for sustainable management of water resources in Turkey, have been briefly introduced with their basic theoretical and numerical backgrounds. HİDROTÜRK model includes three individually processing hydrodynamic sub-models, namely one (1-D), two (2-D), and three (3-D) dimensional written in FORTRAN programming language. Inputs and outputs of all sub-models are managed through a user-friendly interface. The 1-D hydrodynamic model solves the Saint-Venant equations, which are gradually varied unsteady flow equations written in the flow direction. It applies a dynamic wave routine. 2-D hydrodynamic model numerically solves the unsteady depth-averaged continuity and momentum equations. 2-D model is more reliable for shallow waters where the areal extent of the domain is dominant over the vertical or for completely mixed water bodies through the water depth. The 3-D hydrodynamic numerical model solves the unsteady Navier-Stokes equations in three dimensions only with the Boussinesq assumption. When the water body is deep, and variable circulations over the water depth occur, especially in the simulations of wind and density induced flows, the application of the 3-D hydrodynamic model is crucial. The software developments and preliminary tests of the models by SWMM5.0-EXTRAN and Three Dimensional Hydrodynamic, Transport and Water Quality Model -3D have been completed, and the verification studies are still ongoing. Some applications to Demirköprü Dam Lake in the Gediz River Basin are presented to show the input and output structures of hydrodynamic models.

Keywords: *HİDROTÜRK, hydrodynamic model, wave routine, continuity, momentum*

Öz

Bu makalede, Türkiye'de su kaynaklarının sürdürülebilir yönetimi için geliştirilen ilk ulusal hidrolojik, hidrodinamik, hidrojeolojik, su kalitesi ve ekolojik modeli olma özelliğine sahip HİDROTÜRK modeli, hidrodinamik alt-model bileşenleri, temel teorik ve sayısal çözümleme kapasiteleriyle kısaca tanıtılmıştır. HİDROTÜRK modeli, FORTRAN programlama dilinde yazılan, bir (1-B), iki (2-B) ve üç (3-B) boyutlu olmak üzere birbirinden bağımsız olarak çalışabilen üç ayrı hidrodinamik alt model içermektedir. Tüm alt modellerin girdileri ve çıktıları kullanıcı dostu bir

* *Corresponding author*

arayüz üzerinden yönetilmektedir. 1-B hidrodinamik model, akış yönünde yazılan yavaş değişen kararsız akış denklemleri olan Saint-Venant denklemlerini çözmekte ve dinamik dalga ötelemesi uygulamaktadır. 2-B hidrodinamik model, derinlik boyunca ortalaması alınmış, kararsız süreklilik ve hareket denklemlerini sayısal olarak çözümler ve yüzey alanı büyüklüğünün su derinliğine göre çok daha baskın olduğu sığ sular için veya su derinliği boyunca tam karışımlı su kütleleri için daha güvenilir benzeşimler sunar. 3-B hidrodinamik model, kararsız Navier-Stokes denklemlerini yalnızca Bousinessq varsayımı ile üç boyutta sayısal olarak çözümlemektedir. Su kütlesinin derinlikleri fazla olduğunda ve özellikle rüzgar ve yoğunluk kaynaklı çevrintiler gibi su kolonu boyunca yön değiştirebilen akıntıların hesaplanmasında 3-B hidrodinamik modelin kullanılması gereklidir. Modellerin yazılım geliştirmeleri ve SWMM5.0-EXTRAN ve HYDROTAM-3D sayısal modelleri ile karşılaştırmalı ön testleri tamamlanmış, doğrulama çalışmaları ise halen devam etmektedir. Modellerin girdi ve çıktı formatlarını göstermek amacıyla, Gediz Nehri Havzası'ndaki Demirköprü Baraj Gölü için yapılan hidrodinamik model uygulamalarından bazılarına yer verilmiştir.

Anahtar kelimeler: *HİDROTÜRK, hidrodinamik model, dalga öteleme, süreklilik, momentum*

Introduction

Hydrodynamic modeling aims to predict velocity components, flow rates, surface-level changes, pressure gradients, and density variations due to changes in temperature, salinity, and pressure for fluids in motion. The hydrodynamic models have been subdivided into mainly three groups as one dimensional (1-D), two dimensional (2-D), and three dimensional (3-D) models concerning the dimensionality of the physical phenomenon.

Hydrologic Engineering Center-River Analysis System (HEC-RAS) is a model that simulates 1-D and 2-D unsteady flow in open channels and floodplains (Hydrologic Engineering Center [HEC], 2016). Model components include the dam break analysis, levee breaching and overtopping, and pipe flow systems. It can combine 1-D and 2-D unsteady flow modeling.

As the 1-D hydrodynamic model, the Extended Transport Model (EXTRAN) component of the Storm Water Management Model (SWMM), which has been commonly applied all over the world for surface waters, has been adapted (Rossman, 2006, 2015). EXTRAN is written in the FORTRAN language, and it is an open-source code. The code unit system is converted to the International Unit System (SI). Program inputs and outputs are all modified, and a user-friendly interface has been prepared for their management. The user interacts with HİDROTÜRK through a graphical user interface prepared for the 1-D hydrodynamic model. The interface is designed to make it easy to use the software while maintaining a high level of efficiency for the user.

Several 1-D and 2-D hydrodynamic models are developed to simulate the floodwater propagation in floodplain areas (Horritt & Bates, 2002). DHI MIKE 11 is a commonly applied model to simulate complex three-dimensional flow patterns (Thompson et al., 2004). It can handle the effects of many hydraulic structures like culverts, bridges, and dams. The Environmental Fluid Dynamics Code (EFDC) is a model system having hydrodynamic, eutrophication, sediment, and contaminant submodels. EFDC applies to enclosed water bodies, rivers, estuaries, and coastal areas (Hamrick, 1992; Ji et al., 2001).

Three Dimensional Hydrodynamic, Transport and Water Quality Model (HYDROTAM-3D) is the first national 3-D hydrodynamic, transport, and water quality model developed for coastal areas in Turkey. It has been applied to many coastal areas in Turkey to simulate wind, wave, and density induced currents and has been verified with analytical solutions and many site measurements (Balas & Özhan, 2000, 2002; Balas et al., 2012; Cebe & Balas, 2016, 2018; Genç et al., 2020). The model is based on GIS and cloud computing technology, and it includes an extensive database for coastal and estuarine water bodies in Turkey. It has electronic wind and wave climate and energy atlas, wave propagation, sediment transport, coastal morphology, and water quality modules.

Almost all circulation systems in nature have three-dimensional character. Therefore a 3-D hydrodynamic model can be expected to solve all current system behaviors in nature. However, due to the complexity of the turbulence in three-dimensions, they are generally time-consuming, and for some of the flow problems, 3-D numerical modeling would not lead to advantageous solutions and will significantly decrease the processing performance. For example, the investigation of a 500 km long river having a width of 50-200 m with a three-dimensional model is not meaningful, mainly if a local circulation event in the river cross-section is not investigated. Similar if water depths are very shallow, being typically less than 5-10 m, having a horizontal extend in the order of kilometers, use of the depth-averaged 2-D hydrodynamic model will provide reliable results. Therefore, the HİDROTÜRK model includes a 1-D hydrodynamic model to work with long and narrow water bodies, especially for rivers, a 2-D hydrodynamic model for shallow and large water bodies, and a 3-D hydrodynamic model for all other types.

Method

One-Dimensional Hydrodynamic Model

One-dimensional (1-D) hydrodynamic model is a hydraulic flood routing model developed for open channels and closed conduit systems. The open-source module named Extended Transport Model (EXTRAN.f), a 1-D hydrodynamic

module, has been made operational as a one-dimensional hydrodynamic model component of the HIDROTURK model. The model numerically solves the transport equations and calculates the stream from the main drainage line to the outfall node by the dynamic displacement method. The model idealizes the channel/conduit system to links connected to nodes or junctions. Links transmit flow from node to node. The discharge, Q, is the fundamental parameter in the links. The average flow is solved in each link, assuming as constant in a time-step. Nodes are the junctions of links. The cross-sectional flow area, depth, and velocity vary in each link. Any inflows like inlet hydrographs, or outflows, like free outfalls, are defined at each related nodes. The volume, surface area, and total head are the computed variables at the nodes. At every time step of the computations, the volume change is computed that leads to the discharge and total head computations (Roesner et al., 1992). Table 1 presents the elements and their types.

Table 1

Elements and Their Types in 1-D HİDROTURK Model

Elements	Types
Links	Natural (irregular cross section) channel
	Rectangular
	Trapezoidal
	Power function
	Circular
Diversion Structures	Orifice
	Transverse weir
	Side flow weir
	Pump
Storage Basin	Area-stage relationship
	Enlarged tunnels or pipes
Outfall Structures	Transverse weir
	Side flow weir
	Outfall with gate
	Free outfall

When a system is to be analyzed with a 1-D model, the first step is generally to define the system and the watershed that it drains. Each of the sub-basins discharges the currents formed on its surface to a defined drainage channel. It is necessary to place a junction in the drainage routes where backwater effects, surcharge, and diversion facilities affect the flow and head computation. Junction points should be identified as each:

-Upstream terminal point(s) in the system,
-Outfall and discharge point(s),
-Bridges and culverts
-The pump station, storage point, orifice and weir diversion,
-The junction where inflow hydrographs will be input
-Points where pipe/channel size/shape changes significantly,
-Points where pipe/channel slope changes significantly.

The one-dimensional numerical hydrodynamic model solves the conservation of mass and momentum equations, known as the Saint-Venant equations, which are gradually varied, one-dimensional unsteady flow equations:

$$\frac{\partial A}{\partial t}+\frac{\partial Q}{\partial x}=0 \quad (1)$$

$$\frac{\partial Q}{\partial t}+\frac{\partial\left(\frac{Q^2}{A}\right)}{\partial x}+gA\frac{\partial H}{\partial x}+gAS_f=0 \quad (2)$$

where, Q = AV, V: average velocity, A:cross-sectional area, t:time, x:length of the channel or conduit, Q:flow rate, g: gravitational acceleration, H:hydraulic head, S_f: friction slope. The bottom slope is incorporated into gradient of H.

The model uses the momentum equation in the links and a particular lumped continuity equation for the nodes. Thus, momentum is conserved in the links and continuity in the nodes. In the dynamic wave routine, the momentum equation is combined with the continuity giving an equation for a solution along with each link at each time step.

$$\frac{\partial Q}{\partial t}-2V\frac{\partial A}{\partial t}-V^2\frac{\partial A}{\partial x}+gA\frac{\partial H}{\partial x}+gAS_f=0 \quad (3)$$

The model uses the Manning equation to express the relationship between flow rate (Q), cross-sectional area (A), hydraulic radius (R), and slope (S) in all conduits;

$$Q=\frac{1}{n}\ AR^{2/3}\ S^{1/2} \quad (4)$$

Where n is the Manning roughness coefficient and S is the friction slope.

The specific function of the dynamic wave routine is to route inlet hydrographs through the network of pipes, junctions, and flow diversion structures of the main sewer system to the treatment plant interceptors and receiving water outfalls. Dynamic wave routine is used whenever it is crucial to represent surcharged or severe backwater conditions and special flow devices or structures such as weirs, orifices, pumps, storage basins, culverts, bridges, and gates. The routine can simulate pipes, manholes (pipe junctions), weirs, orifices, pumps, storage basins, and outfall structures. Typically in flow routing, when the flow into a junction exceeds the system's capacity to transport it further downstream, the excess volume overflows the system and is lost. An option exists to have the excess volume instead be stored atop the junction, in a ponded fashion, and be reintroduced into the system as capacity permits. Under steady and kinematic wave flow routing, the ponded water is stored simply as an excess volume. For dynamic wave routing, which is influenced by the water depths maintained at nodes, the excess volume is assumed to pond over the node with a constant surface area. This amount of surface area is an input parameter supplied for the junction. Alternatively, the user may wish to represent the surface overflow system explicitly. In open channel systems, this can include road overflows at bridges or culvert crossings as well as additional floodplain storage areas. 1D model calculations produce the output required for flooding analysis.

The input data of the 1-D hydrodynamic model is divided into 23 groups. 1-6 groups include control data that determines time step, start time, junction points with hydrograph input, junctions, and conduits for printing heads and flows. The identification of conduits and junctions is made in data groups 7-8. Groups 9-12 contain data for account points with storage, orifice, sluice, and pump. 13-17 groups define the discharge points and associated backwater conditions. Groups 18-19 define the initial flowrate and heads at the calculation points. Groups 20-21 provide hydrographs, and groups 22-23 define the properties of bridges and culverts.

Figure 1 shows nodes and links defining some tributaries of the Gediz River, as obtained from the HİDROTÜRK interface. Points define the nodes, and lines define the links.

Figure 1

Nodes (Blue Points) and Links (Yelow Lines) that Define Some Tributaries of the Gediz River

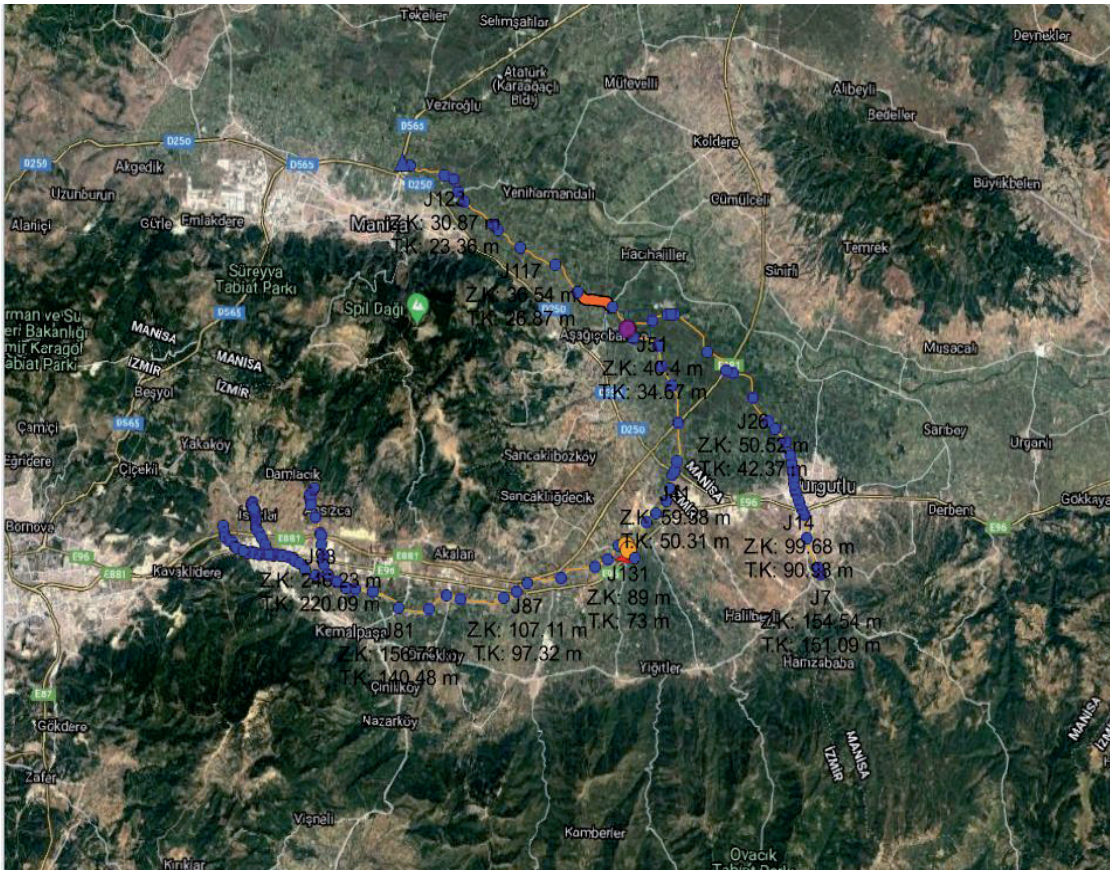

Most open channels are represented with a trapezoidal, rectangular, or irregular cross-sections. For a user-defined irregular natural channel, the cross-sectional stations have to be defined with the variable depth (y) and the distance across the cross-section (x). A typical natural channel cross-section defined in the HİDROTÜRK model having a bridge is given in Figure 2.

Figure 2

A Typical Natural Channel Cross-Section with a Bridge

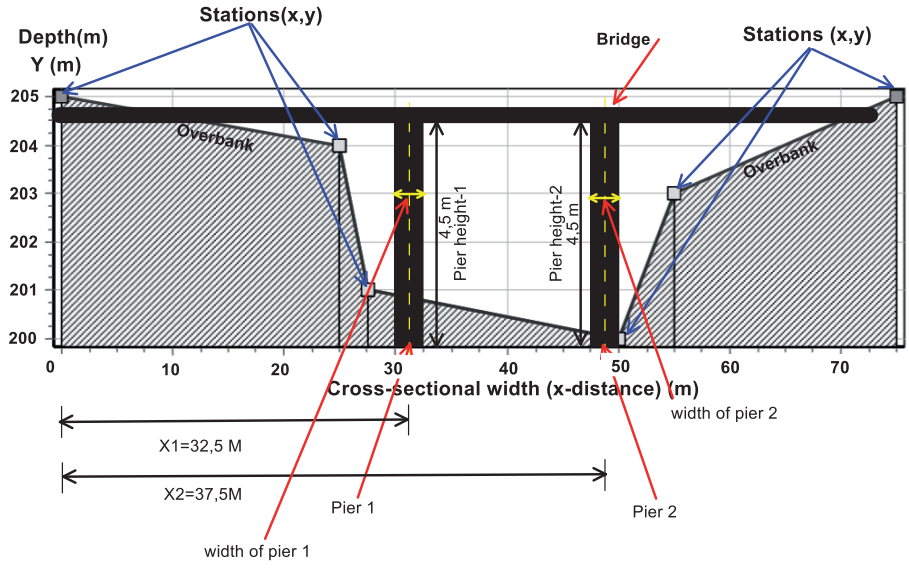

Two Dimensional Hydrodynamic Model

In relatively shallow waters, there is no significant stratification in vertical, and hydrodynamic properties do not vary over depth. Therefore water particle velocities in horizontal directions are calculated by shallow water equations. In the two dimensional hydrodynamic sub-model of HİDROTÜRK, the continuity equation is given as;

$$\frac{\partial \eta}{\partial t}+\frac{\partial Hu}{\partial x}+\frac{\partial Hv}{\partial y}=0 \tag{5}$$

The momentum equations in x and y directions are;

$$\frac{\partial u}{\partial t}+u\frac{\partial u}{\partial x}+v\frac{\partial u}{\partial y}-fv=-g\frac{\partial \eta}{\partial x}+\frac{\left(\tau_x^{sur}-\tau_x^{bot}\right)}{\rho_w H}+\upsilon_t^H\left(\frac{\partial^2 u}{\partial x^2}+\frac{\partial^2 u}{\partial y^2}\right) \tag{6}$$

$$\frac{\partial v}{\partial t}+u\frac{\partial v}{\partial x}+v\frac{\partial v}{\partial y}+fu=-g\frac{\partial \eta}{\partial x}+\frac{\left(\tau_y^{sur}-\tau_y^{bot}\right)}{\rho_w H}+\upsilon_t^H\left(\frac{\partial^2 v}{\partial x^2}+\frac{\partial^2 v}{\partial y^2}\right) \quad (7)$$

In these equations; x and y: distances in horizontal plane; t: time; u and v: velocities in x and y directions, respectively; H: water depth, f: Coriolis parameter, υ_t^H:Eddy viscosity in horizontal, η: water surface level, ρ_w: density of water, τ_x^{sur}ve τ_y^{bot} :shear stress in x and y directions at the surface and at the bottom respectively. Shear stresses at the surface and bottom are calculated as in the followings:

$$\tau_x^{sur}=C_D\rho_a|U_w|U_w \; ; \; \tau_y^{sur}=C_D\rho_a|V_w|V_w \quad (8)$$

$$\tau_x^{bot}=C_B\rho_w|u|u \; ; \; \tau_y^{bot}=C_B\rho_w|v|v \quad (9)$$

In these equations, U_w and V_w:effective wind speeds in x and y directions respectively; ρ_a: air density; C_D and C_B wind factor and bottom friction coefficients respectively.

The 2-D advection-diffusion equation for the transport of salinity and temperature is given as;

$$\frac{\partial C}{\partial t}+u\frac{\partial C}{\partial x}+v\frac{\partial C}{\partial y}=\frac{\partial}{\partial x}\left(D_x\frac{\partial C}{\partial x}\right)+\frac{\partial}{\partial y}\left(D_y\frac{\partial C}{\partial y}\right)\pm S_c \quad (10)$$

where C is temperature (T) or salinity (S) concentration, D_x, D_x are turbulent diffusion coefficients and S_c is any source or sink terms in the computational domain (Tunaboylu, 2006).

The solution algorithms are similar to the three-dimensional model that will be explained below in detail.

Three Dimensional Hydrodynamic Model

In three dimensional hydrodynamic model, 3-D Navier-Stokes Equations are solved numerically in Cartesian coordinates as depicted in Figure 3 (Balas & Özhan, 2000).

Figure 3

Cartesian Coordinate System

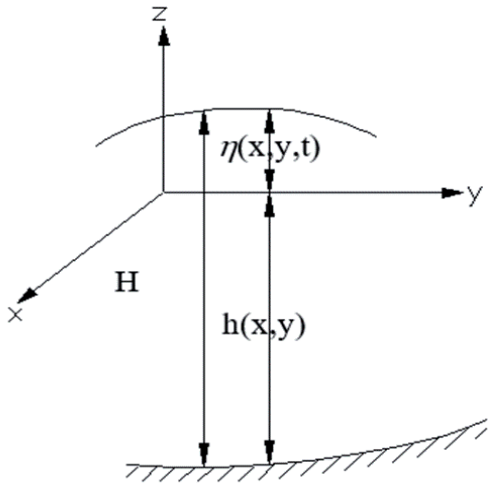

Model equations are given below.

Continuity equation;

$$\frac{\partial u}{\partial x}+\frac{\partial v}{\partial y}+\frac{\partial w}{\partial z}=0 \tag{11}$$

Momentum equations in x, y and z directions that are perpendicular to each other on a horizontal plane;

$$\frac{\partial u}{\partial t}+u\frac{\partial u}{\partial x}+v\frac{\partial u}{\partial y}+w\frac{\partial u}{\partial z}=fv-\frac{1}{\rho_o}\frac{\partial p}{\partial x}+2\frac{\partial}{\partial x}\left(\nu_x\frac{\partial u}{\partial x}\right)+\frac{\partial}{\partial y}\left(\nu_y\left(\frac{\partial u}{\partial y}+\frac{\partial v}{\partial x}\right)\right)+\frac{\partial}{\partial z}\left(\nu_z\left(\frac{\partial u}{\partial z}+\frac{\partial w}{\partial x}\right)\right) \tag{12}$$

$$\frac{\partial v}{\partial t}+u\frac{\partial v}{\partial x}+v\frac{\partial v}{\partial y}+w\frac{\partial v}{\partial z}=-fu-\frac{1}{\rho_o}\frac{\partial p}{\partial y}+\frac{\partial}{\partial x}\left(\nu_x\left(\frac{\partial v}{\partial x}+\frac{\partial u}{\partial y}\right)\right)+2\frac{\partial}{\partial y}\left(\nu_y\frac{\partial v}{\partial y}\right)+\frac{\partial}{\partial z}\left(\nu_z\left(\frac{\partial v}{\partial z}+\frac{\partial w}{\partial y}\right)\right) \tag{13}$$

$$\frac{\partial w}{\partial t}+u\frac{\partial w}{\partial x}+v\frac{\partial w}{\partial y}+w\frac{\partial w}{\partial z}=gz-\frac{1}{\rho_o}\frac{\partial p}{\partial z}+\frac{\partial}{\partial x}\left(\nu_x\left(\frac{\partial w}{\partial x}+\frac{\partial u}{\partial z}\right)\right)+\frac{\partial}{\partial y}\left(\nu_y\left(\frac{\partial w}{\partial y}+\frac{\partial v}{\partial z}\right)\right)+2\frac{\partial}{\partial z}\left(\nu_z\frac{\partial w}{\partial z}\right) \quad (14)$$

In these equations; (x, y) and z: horizontal and vertical coordinates respectively; t: time; u, v, w: velocity components in x, y and z directions on any grid point; ν_x, ν_y, ν_z: eddy viscosities in x, y and z directions respectively; f: Corriolis coefficient, $\rho(x,y,z,t)$: water density, g: gravitational acceleration, p: pressure.

The water's density varies with its salinity and temperature by the following equations (Gill, 1982).

$$C(h)=999.83+5.053h-0.048h^2$$
$$\beta(h)=0.808-0.0085h$$
$$\alpha(T,h)=0.0708(1+0.351h+0.068(1-0.0683h)T)$$
$$\gamma(T,h)=0.003(1-0.059h-0.012(1-0.064h)T)$$
$$\rho=C(h)+\beta(h)S-\alpha(T,h)-\gamma(T,h)(35-S)(13) \quad (15)$$

Where S is salinity (%), h is depth of water (km) and T is temperature (°C).

The temperature and salinity changes are computed from three-dimensional advection-diffusion equations (Balas & Özhan, 2000).

$$\frac{\partial C}{\partial t}+u\frac{\partial C}{\partial x}+v\frac{\partial C}{\partial y}+w\frac{\partial C}{\partial z}=\frac{\partial}{\partial x}\left(D_x\frac{\partial C}{\partial x}\right)+\frac{\partial}{\partial y}\left(D_y\frac{\partial C}{\partial y}\right)+\frac{\partial}{\partial z}\left(D_z\frac{\partial C}{\partial z}\right)\pm S_c \quad (16)$$

Where C is the temperature (T) or salinity (S) concentration, D_x, D_x, and D_z are turbulent diffusion coefficients, and S_c is any source or sink terms in the computational domain. The heat exchange boundary condition is modified to consider a heat flux from the atmosphere. In the baroclinic circulations, consideration of heat exchange might be valuable in the vertical convective term (Balas & Özhan, 2002).

The kinematic surface boundary condition depends on the water level change as defined in Equation (17).

$$\frac{\partial \eta}{\partial t}+u_s\frac{\partial \eta}{\partial x}+v_s\frac{\partial \eta}{\partial y}-w_s=0 \quad (17)$$

Here; u_s and v_s: horizontal velocity components at the surface; w_s: vertical velocity component at the surface; η: water level change. The definitions of water surface and water depth are given in Figure 3 in a 3-D Cartesian coordinate system.

The continuity equation is integrated over the water depth, and the surface kinematic boundary condition is applied to obtain the water level change equation (η) as given below:

$$\frac{\partial \eta}{\partial t}+\frac{\partial}{\partial x}\left[\int_{-h}^{\eta} u\,dz\right]+\frac{\partial}{\partial y}\left[\int_{-h}^{\eta} v\,dz\right]=0 \quad (18)$$

where; h(x, y): water depth according to still water level. H(x, y, t): Total water depth and given as H(x, y, t)=h(x, y)+η (x, y, t). The momentum equations are subject to the vertical exchange of momentum at the free surface due to the wind stress and at the bottom due to the bottom stress. Thus at the surface,

$$\tau_x^s=\tau_x^w=C_D\rho_a|W|W_x=\rho\nu_z\frac{\partial u}{\partial z} \quad \text{and} \quad \tau_y^s=\tau_y^w=C_D\rho_a|W|W_x=\rho\nu_z\frac{\partial v}{\partial z} \quad (19)$$

where ρ_a is air density, W is wind velocity and C_D is wind drag coefficient.

The bottom boundary condition is as follows:

$$w=-u_b\frac{\partial h}{\partial x}+v_b\frac{\partial h}{\partial y} \quad (20)$$

If any open boundary condition exists, the radiation boundary condition is applied. The land boundary conditions are usually taken as no flux. The numerical solution is based on finite differences on a staggered scheme, as shown in Figure 4.

Figure 4

Staggered Scheme Applied in Numerical Solution

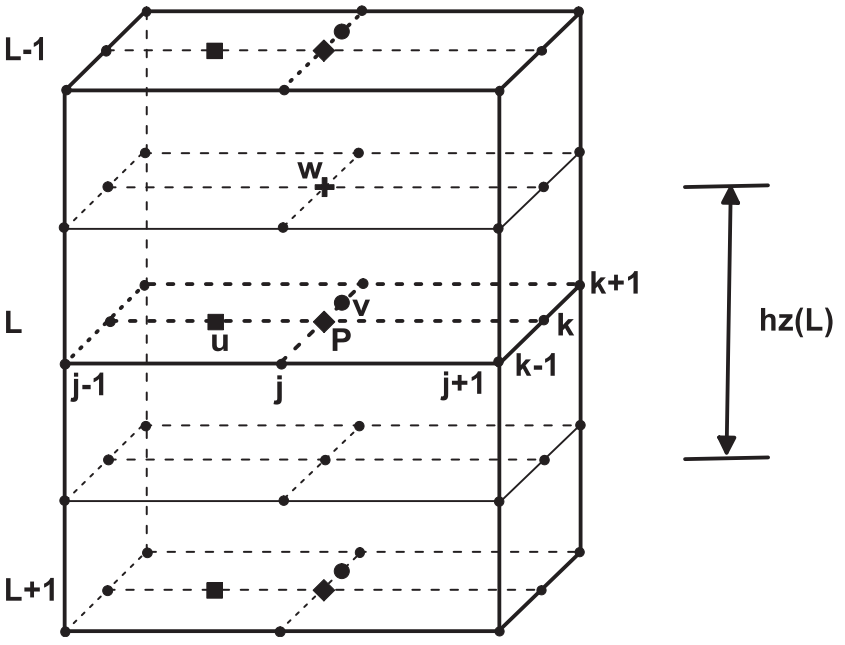

The indices along x, y and z directions are j, k, and L, respectively. The grid distances along x and y directions are constant, whereas the hz (L) denotes the grid-distance along the z-direction, which is a variable. The starting point of the coordinate system is located at the free surface, and the z-axis points upward. Therefore, as the depth becomes negative, hz (L) becomes positive.

The use of constant layer thickness in the vertical processes causes inefficient processes, especially if there are abrupt variations in the topography. A dimensionless coordinate is introduced through the sigma coordinate transformation to overcome these instabilities. The vertical coordinate has been stretched; thus, the vertical grid size is expressed as a function of the computational grid depth, with the sigma coordinate transformation (Kowalik & Murty, 1993). The new coordinate defined is expressed as;

$$\sigma = \frac{z - \eta}{h + \eta} \tag{21}$$

Along with the water depth, sigma coordinate transformation has been applied to follow the bottom topography. The total depth h+η is denoted as H. The water column (from the surface where z = η to the bottom where z = -H) is transformed into a uniform depth ranging from σ=0 to σ=-1. After the application of transformation, there would be the same number of vertical layers over the whole computational domain, and created mesh follows the contours of the variable topography, as shown in Figure 5.

Figure 5

Variable Vertical Mesh with The Application of Sigma Coordinate Transformation

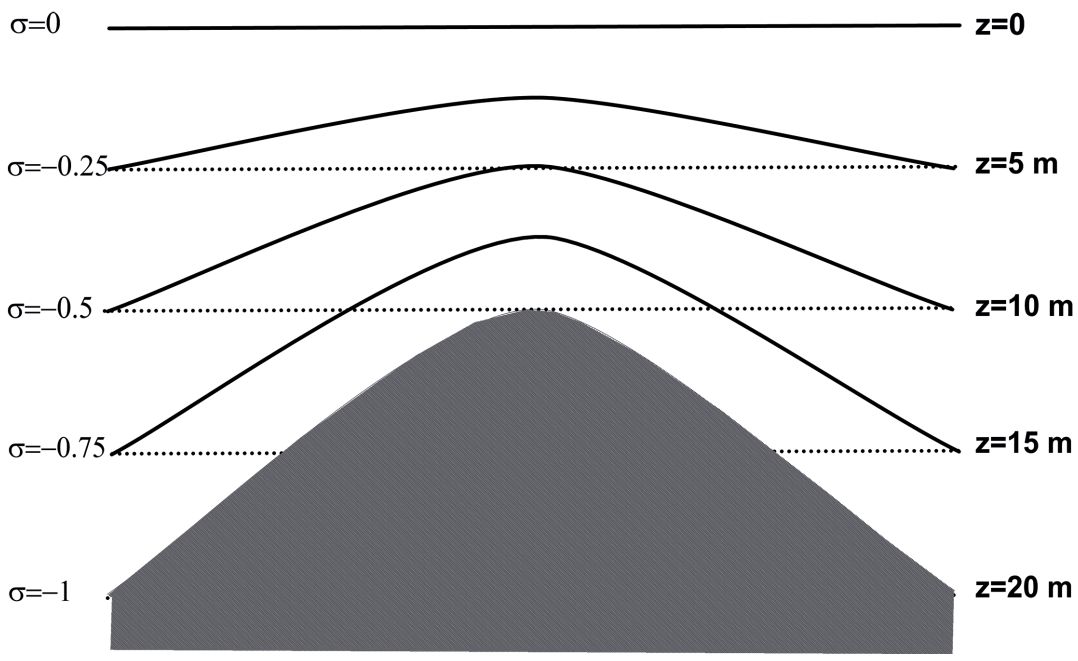

The sigma coordinate transformation not only changes the vertical direction, but it also affects the horizontal coordinates. All partial derivatives in equations solved are corrected according to the transformed system of coordinates. The derivative of any dependent variable f in the basic equations with respect to the vertical coordinate z is:

$$\frac{\partial f}{\partial z}=\frac{1}{H}\frac{\partial f}{\partial \sigma} \qquad (22)$$

Derivative of any dependent variable f in the basic equations with respect to the horizontal coordinate x is:

$$\frac{\partial f}{\partial x}=\frac{\partial f}{\partial x}\Big|_{\sigma}-\frac{1}{H}\left(\sigma\frac{\partial H}{\partial x}+\frac{\partial \eta}{\partial x}\right)\frac{\partial f}{\partial \sigma} \tag{23}$$

So all the basic equations are transformed into sigma coordinates before the application of finite difference approximations. For example, the continuity equation takes the following form:

$$\frac{\partial u}{\partial x}+\frac{\partial v}{\partial y}+\frac{\partial w}{\partial z}=\frac{\partial u}{\partial x}-\frac{1}{H}\frac{\partial(H\sigma+\eta)}{\partial x}\frac{\partial u}{\partial \sigma}+\frac{\partial v}{\partial y}-\frac{1}{H}\frac{\partial(H\sigma+\eta)}{\partial y}\frac{\partial v}{\partial \sigma}+\frac{1}{H}\frac{\partial w}{\partial \sigma} \tag{24}$$

A two-time-level scheme is used in time-wise solutions of equations. The first time step, from t to t∗, uses an explicit scheme to compute the variables' predictive values. At the second time step, from t∗ to t+1, an implicit scheme is applied to ensure dynamic stability.

The finite-difference approximations of second-order for space differencing are applied to the staggered scheme, as shown in Figure 6. The total depth is defined in all (j, k, L) points, while the above equations require all the depths in u and v points on a staggered scheme. Therefore, depths are calculated at u and v computational points and defined as HU and HV (Kowalik & Murty, 1993).

$$HU_{j,k}=0.5*(H_{j,k}+H_{j-1,k}) \text{ and } HV_{j,k}=0.5*(H_{j,k}+H_{j,k+1}) \tag{25}$$

Each term in the equations is expressed considering its position defined on the staggered scheme applied. For example, when the nonlinear advective term in the x direction of x-momentum equation, $\frac{\partial}{\partial x}(u^2H)$ is considered; first the average value of term is calculated at the depth points where surface elevation (η) is calculated which surround u point, and then diff erence for the derivative is applied according to scheme given in Figure 4 and Figure 6. These η points are indexed by (j, k, L) and (j −1, k, L), respectively. At the right η and at the left of grid point average values are given as;

$(UH)_r=0.5(HU_{j+1,k}*u_{j+1,k,L}+HU_{j,k}*u_{j,k,L})$ $\quad u_r=0.5(u_{j,k,L}+u_{j+1,k,L})$

$(UH)_l=0.5(HU_{j-1,k}*u_{j-1,k,L}+HU_{j,k}*u_{j,k,L})$ $\quad u_l=0.5(u_{j,k,L}+u_{j-1,k,L})$

So, the derivative of the term is calculated by Eq.(26).

$$\frac{\partial}{\partial x}(u^2H)=\frac{(uH)_r*u_r-(uH)_l*u_l}{hx} \tag{26}$$

As an example along the y direction derivatives in x-momentum equation, the advective term $\frac{\partial}{\partial y}(uvH)$ is expressed using all variables located up and down of the point $u_{j,k,L}$ as shown in Figure 7.

$(vH)_{up}=0.5(HV_{j,k}*v_{j,k,L}+HV_{j-1,k}*v_{j-1,k,L})$ $\quad u_{up}=0.5(u_{j,k,L}+u_{j,k+1,L})$

$(vH)_{down}=0.5(HV_{j,k-1}*v_{j,k-1,L}+HV_{j-1,k-1}*v_{j-1,k-1,L})$ $\quad u_{down}=0.5(u_{j,k,L}+u_{j,k-1,L})$

$$\frac{\partial}{\partial y}(uvH)=\frac{(vH)_{up}*u_{up}-(vH)_{down}*u_{down}}{hy} \tag{27}$$

Figure 6

Staggered Scheme Used in X Differencing Computations

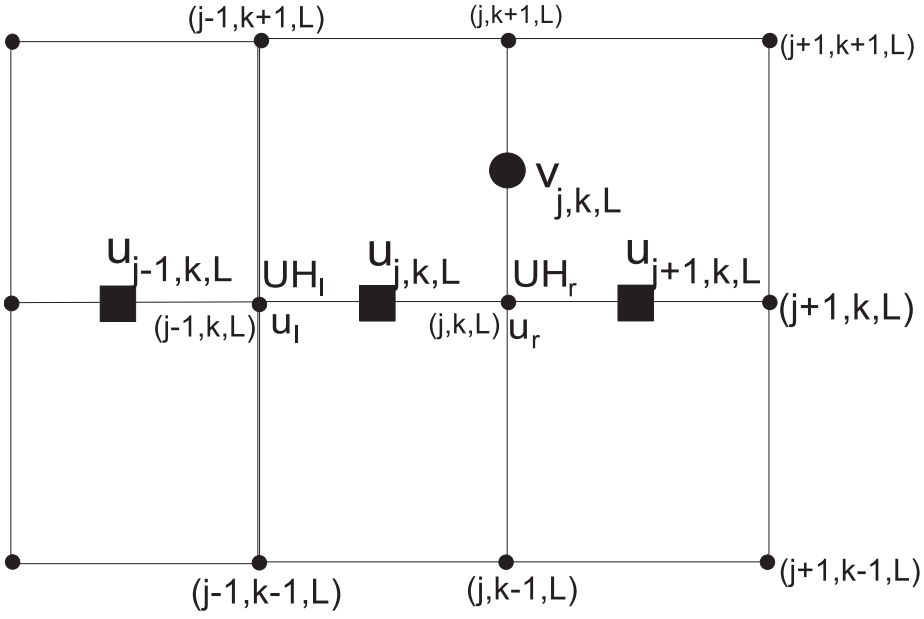

Figure 7

Staggered Scheme Used in Y Differencing Computations

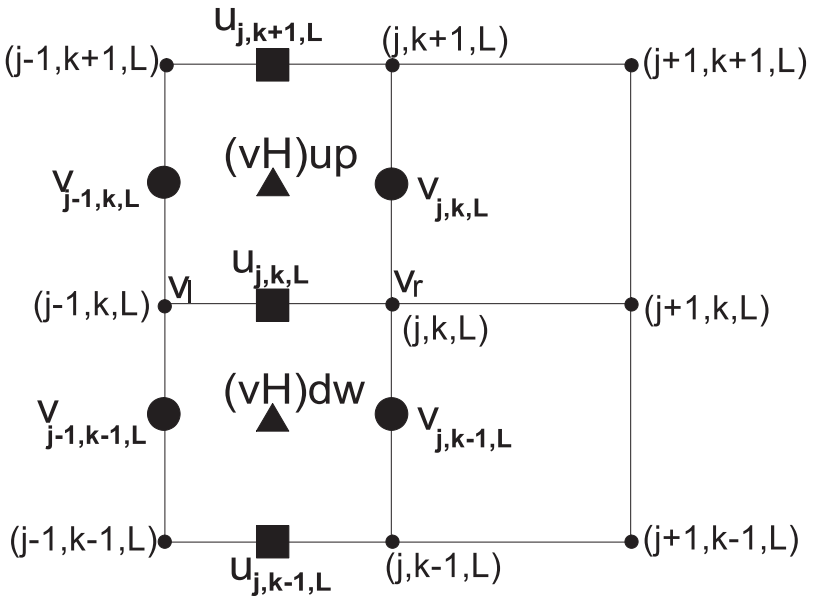

For the nonlinear convective transport term in vertical $\frac{\partial}{\partial\sigma}(wu)$ in x-momentum equation, the derivative based on the values above and below the u grid point is constructed. Since vertical velocity w is not located above the u grid, but above pressure P grid point as shown in Figure 4, the averaging is performed considering the location of $u_{j,k,L}$ grid point.

$w_{above}=0.5(w_{j,k,L}+w_{j-1,k,L})$ $\quad$ $w_{below}=0.5(w_{j,k,L+1}+w_{j-1,k,L+1})$

$u_{above}=(u_{j,k-1,L}*hz_L+u_{j,k,L}*hz_{L-1})/(hz_L+hz_{L-1})$

$u_{below}=(u_{j,k,L}*hz_{L+1}+u_{j,k,L+1}*hz_L)/(hz_L+hz_{L+1})$

$$\frac{\partial}{\partial\sigma}(wu)=(u_{above}*w_{above}-u_{below}*w_{below})/hz_L \quad (28)$$

Similarly, all related differencing approximations are applied considering the related computational points on staggered scheme shown in Figure 4.

Results

The developed hydrodynamic models are applied to the Gediz River basin during their testing process. In this section, the input and output structures of the models are aimed to be presented rather than the flow investigations. 1-D hydrodynamic model application to some of the tributaries of the Gediz River have been shown in Figure 8. The links (L) and nodes (J) that the changes of water surface profile, flow rate, flow velocity, and depth of water have been investigated, are selected from the map using the model interface. The time-wise water level changes over the cross-section or along the flow direction have been animated and graphically shown for the selected links or nodes. As an example, the change of water surface level is shown for the selected junction (node) J84 marked by a yellow point in Figure 8 over its natural cross-section. On the graph, the interface presents a change of water depth in time at every interested time step of output over the model's total run time. In this manner, change of water depth can be observed on the selected node cross-section in a time-wise animated manner. Likewise, the longitudinal profile of the selected links can be obtained in time-wise animation. In Figure 9, the longitudinal water depth profile of links between nodes J83 and J85, namely for L78 and L79, are presented. In both of the figures, the red line shows the maximum water level elevations that are reached during the run time.

Meanwhile, maximum water surface elevation also shows the possible flooding that might occur out of the main natural channel towards the flooding plains. It is rather easy to observe flooding plains in cross-sectional graphs. Red circles indicate the left and right overbank channel starting points on the graph (Figure 8). So the cross-sectional overbank flow information is also provided in longitudinal profiles, as shown in Figure 9, by inserting the left and right overbank points indicated by light and dark grey lines, respectively. Frequently the left and right overbank elevations on both sides of the channel are not equal to each other (Figure 8), so the lower one is used to indicate the beginning of the overbank flow. If at any time step of the computations the maximum water depth level exceeds the overbank elevations, there occurs the overbank flow.

The first step in the application of 2-D and 3-D hydrodynamic models is to input the bathymetry. The second step is to define the computational domain. The numerical grid is created for Demirköprü Dam Lake, as shown in Figure 10 by the user, stating the wet and dry cell initially. A zero water depth characterizes dry cells, whereas wet cells have a specific water depth below the surface.

Figure 8

Change of Water Depth in the Natural Channel Cross-Section at Node J84 at the End of 11 Days of Run Time

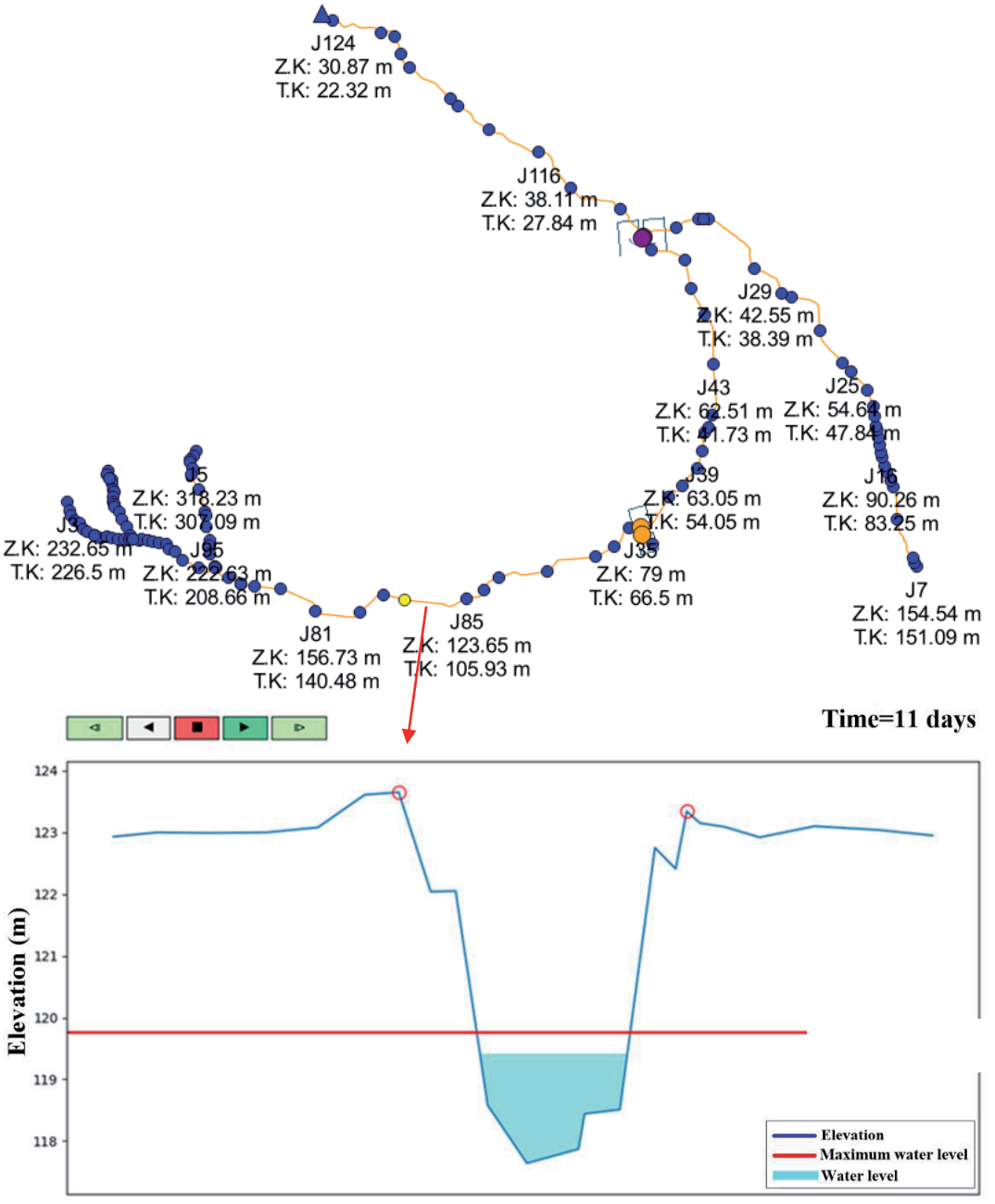

Figure 9

Longitudinal Profile of Water Depth between Nodes J83-J85 at the End of 7 Days

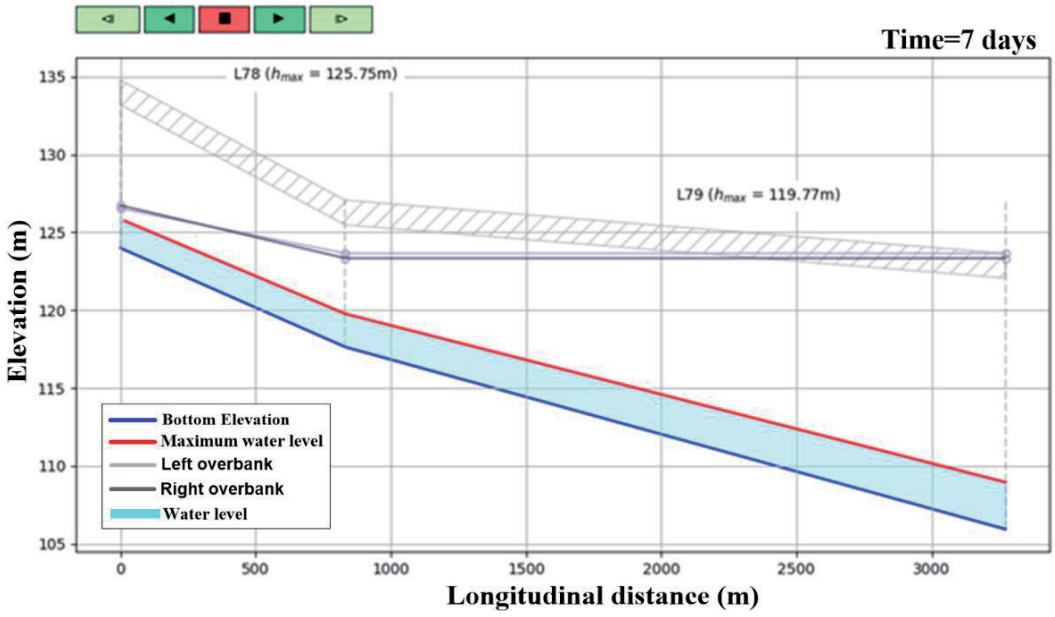

Figure 10

Computational Grid System for Demirköprü Dam Lake (Blue Dot: Wet Cell, Red Dot: Dry Cell)

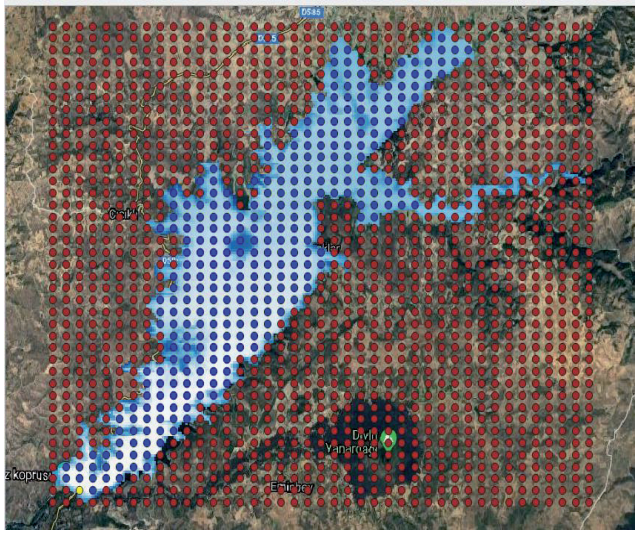

Wind force that drags the surface waters is defined with wind speed, wind direction, and wind duration in a time series over the run time. Initial values of all the variables in the fundamental equations (v, u, w, T, S, and H) are defined over the mesh system. If inflows are discharging into the system or outflows leaving the system, they are specified as hydrographs at the concerned boundary points as boundary conditions. If at certain boundaries, surface water level changes as a function of time are recorded or simulated by other means, they are specified as boundary conditions at the corresponding nearest mesh points.

2-D and 3-D hydrodynamic models of HİDROTÜRK are applied to Demirköprü Dam Lake on the Gediz River Basin. Simulations have been performed by the 2-D hydrodynamic model to obtain the average circulation pattern in the Lake. In the model, surface waters are under the influence of the wind blowing continuously from North Northeast (NNE) with a speed of 4 m/s that is the dominant wind effect for the area (HYDROTAM-3D, 2020). Hydrodynamic models successfully simulate the areal and time-wise changes of the velocity components, water level changes, temperature, and salinity distributions. The average circulation pattern and water level changes simulated at the end of one day by the 2-D hydrodynamic model are shown in Figure 11.

Figure 11

Depth Averaged Velocity Pattern at the Surface Layer and Change of Water Level (HİDROTÜRK-2D Hydrodynamic Model)

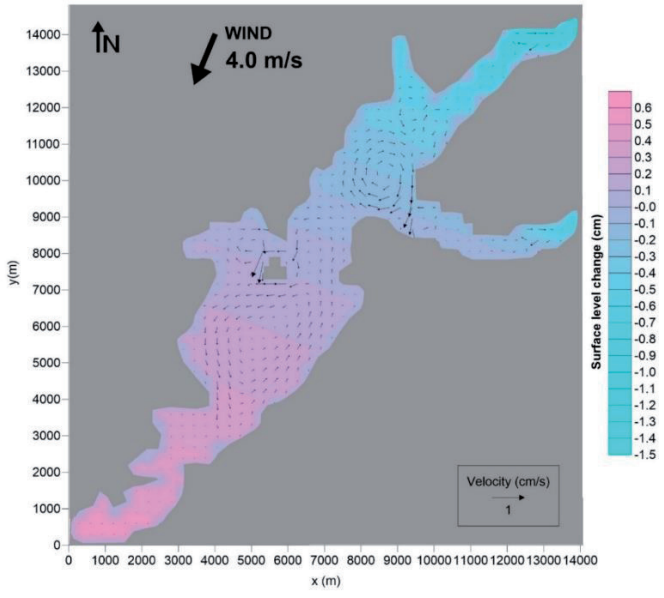

The 3-D hydrodynamic model simulates model parameters at every vertical layer. In 3-D case studies, water depth is divided into six layers following the bottom topography. The velocity pattern at the surface layer and bottom layers of Demirköprü Dam Lake at the end of the one-day simulation are presented in Figure 12 and Figure 13, respectively. Patterns are typical for wind-induced that is surface waters are dragged in the wind direction where there occurs a reverse circulation towards the bottom layers. Figure 14 presents the depth-averaged velocity pattern obtained by averaging the results over the depth and the changes in surface level. It is seen that the average velocity patterns by 2-D and 3-D simulations successfully support each other, predicting the main gyres in the Lake almost at the same locations.

Figure 12

Velocity Pattern at the Surface Layer (HİDROTÜRK-3D Hydrodynamic Model)

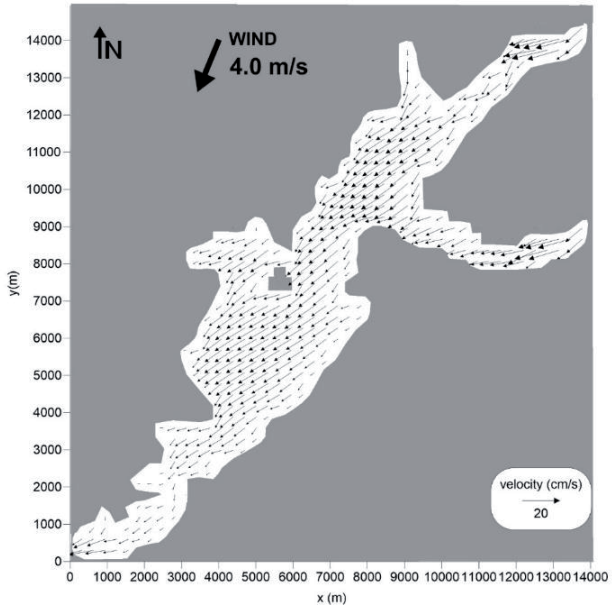

Figure 13

Velocity Pattern at the Bottom Layer (HİDROTÜRK-3D Hydrodynamic Model)

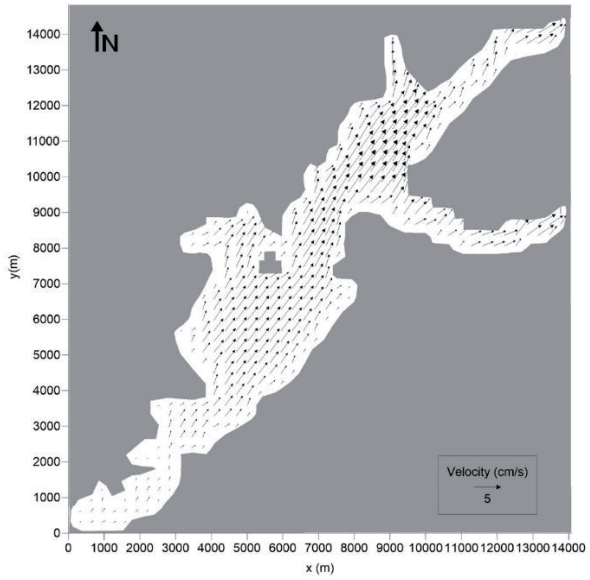

Figure 14

Depth Averaged Velocity Pattern at the Surface Layer and Change of Water Level (HİDROTÜRK-3D Hydrodynamic Model)

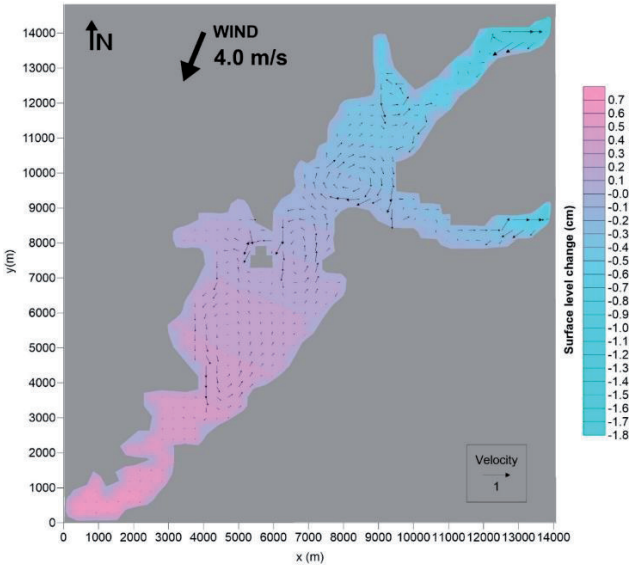

Conclusion

The HİDROTÜRK model is developed under the scope of the project "Development of Hydrological, Water Quality, and Ecological Modeling Tools for Sustainable Management of Water Resources in Turkey." The development of such an integrated model, including hydrological, hydrodynamic, hydrogeological, water quality, and ecological models, is significant and remarkable for the sustainable management of water resources in Turkey. The hydrodynamic model simulations are crucial for the other transport models since the turbulence and velocity patterns mainly control the advection and diffusion processes. Therefore, the degree of accuracy of the transport models is directly related to the hydrodynamic models.

HİDROTÜRK model includes 1-D, 2-D, and 3-D dimensional hydrodynamic models that can work individually or integrated. That is, the outputs of 1-D and 2-D models can be the inputs of the 3-D model. Inputs and outputs of the models are controlled and managed by a user-friendly interface to minimize possible errors that might be due to the user. The software developments and preliminary model tests by SWMM5.0-EXTRAN and HYDROTAM-3D have been successfully completed, and verification studies are still going on. At this stage, the long term and simultaneous site measurements of hydrodynamic and quality parameters at the river basins in Turkey become very important.

Acknowledgement

This work is completed under the scope of the project entitled "Development of Hydrological, Water Quality and Ecological Modeling Tools For Sustainable Management of Water Resources In Turkey," directed by İTÜNOVA Technology I.C. and supported by Republic of Turkey Ministry of Agriculture and Forestry.

References

Balas, L. & Özhan, E. (2000). An implicit three dimensional numerical model to simulate transport processes in coastal water bodies. *International Journal for Numerical Methods in Fluids*, *34*, 307-339.**https://doi.org/10.1002/1097-0363(20001030)34:4%3C307::AID-FLD63%3E3.0.CO;2-T**

Balas, L. & Özhan, E. (2002). Three dimensional modelling of stratified coastal waters. *Estuarine, Coastal and Shelf Science, 54*(1) ,75-87. **https://doi.org/10.1006/ecss.2001.0832**

Balas L., Genç, A.N., & İnan, A. (Eds.).(2012). International Environmental Modelling and Software Society (iEMSs) 2012 International Congress on Environmental Modelling and Software. Managing Resources of a Limited Planet: Pathways and Visions under Uncertainty, Sixth Biennial Meeting, Leipzig, Germany. **http://www.iemss.org/society/index.php/iemss-2012-proceedings**

Cebe, K. & Balas, L. (2016). Water quality modelling in Kaş Bay. *Applied Mathematical Modelling*. , *40*(3),1887-1913. **DOI: 10.1016/j.apm.2015.09.037**

Cebe, K. & Balas, L. (2018). Monitoring and modeling land-based marine pollution. *Regional Studies in Marine Science, 24*, 23-39. **DOI: 10.1016/j.rsma.2018.06.010**

Genç, A.N., Vural, N. & Balas, L. (2020). Modeling transport of microplastics in enclosed coastal waters: A case study in the Fethiye Inner Bay. *Marine Pollution Bulletin*,*150*, 110747. **https://doi.org/10.1016/j.marpolbul.2019.110747**

Gill, A.E. (1982). *Atmosphere-Ocean Dynamics*. International Geophysics Series (Vol.30). Academic Press. **https://www.elsevier.com/books/atmosphere-ocean-dynamics/gill/978-0-12-283522-3.**

Hamrick, J. M. (1992). "*A Three-Dimensional Environmental Fluid Dynamics Computer Code: Theoretical and Computational Aspect"s*. Special Report No. 317 in Applied Marine Science and Ocean Engineering, Virginia Institute of Marine Science School of Marine Science, USA. **https://doi.org/10.21220/V5TT6C**

Hydrologic Engineering Center. (2016). *HEC-RAS user's manuel*. **https://www.hec.usace.army.mil/software/hec-ras/documentation/HEC-RAS_6.0_UsersManual.pdf**

Horritt, M.S., & Bates, P.D. (2002) "Evaluation of 1-D and 2-D numerical models for predicting river flood inundation". *Journal of Hydrology*, *268*(1–4), 87–99. **https://doi.org/10.1016/S0022-1694(02)00121-X**

HYDROTAM-3D (2020). *Three Dimensional Hydrodynamic, Transport and Water Quality Model*. DLTM Limited. **http://www.hydrotam.com**

Ji, Z.G., Morton, M. R., & Hamrick, J. M. (2001). Wetting and drying simulation of estuarine processes. Estuarine, *Coastal and Shelf Science*, *53*(5), 683-700. **https://doi.org/10.1006/ecss.2001.0818**

Kowalik, Z., & Murty, T. S. (1993). *Numerical modeling of ocean dynamics, advanced series on ocean engineering* (Vol.5). World Scientific Publishing. **https://doi.org/10.1142/1970**

Roesner, L. A., Aldrich, J. A., & Dickinson, R. E. (1988). *Storm Water Management Model User's Manual Version 4: Extran Addendum*. US Environmental Protection Agency, Athens, GA. **https://nepis.epa.gov/Exe/ZyPDF.cgi/9101XYKB.PDF?Dockey=9101XYKB.PDF**

Rossman, L. A. (2006). *Storm water management model qualıty assurance report: Dynamic wave flow routing.* U.S. Environmental Protection Agency . **https://nepis.epa.gov/Exe/ZyPDF.cgi/P10089TF.PDF?Dockey=P10089TF.PDF**

Rossman, L.A. (2015). *Stormwater management model reference manual, volume-I hydrology*. U.S. Environmental Protection Agency,. **http://new.streamstech.com/wp-content/uploads/2018/07/SWMM- Reference-Manual-Part-I-Hydrology-1.pdf**

Thompson, J. R., Sørenson, H. R., Gavin, H., & Refsgaard, A. (2004). Application of the coupled MIKE SHE/MIKE 11 modelling system to a lowland wet grassland in southeast England. *Journal of Hydrology*, *293*(1–4),151–179. **https://doi.org/10.1016/j.jhydrol.2004.01.017**

Tunaboylu, S. (2006). *Yoğunluk kaynaklı akıntıların sayısal modellemesi* (180180) [Master's thesis, Gazi University]. **https://tez.yok.gov.tr/UlusalTezMerkezi/tezSorguSonucYeni.jsp**

Extended Turkish Abstract
(Genişletilmiş Türkçe Özet)

HİDROTÜRK Modeli Kullanılarak Hidrodinamik Modelleme

Bu makalede, Türkiye'de su kaynaklarının sürdürülebilir yönetimi için geliştirilen ilk ulusal hidrolojik, su kalitesi ve ekolojik modeli olma özelliğine sahip HİDROTÜRK modeli, hidrodinamik alt-model bileşenleri, temel teorik ve sayısal çözümleme kapasiteleri ile kısaca tanıtılmıştır. Hidrodinamik modellerin başarısı, türbülans benzeşimine ve taşınıma bağlı diğer tüm modellerin başarısını doğrudan etkilemektedir. Bu nedenle hidrodinamik modelleme, bütünleşik sayısal su kalitesi modellemelerinin en önemli bileşenidir. HİDROTÜRK modeli, FORTRAN programlama dilinde yazılan, bir (1-B), iki (2-B) ve üç (3-B) boyutlu olmak üzere, birbirinden bağımsız olarak çalışabilen, üç ayrı hidrodinamik alt model içermektedir. Tüm alt modellerin girdileri ve çıktıları kullanıcı dostu bir arayüz üzerinden yönetilmektedir. Geliştirilen hidrodinamik modeller istenildiği zaman bir arada da çalışabilmektedir. 1-B hidrodinamik modelin çıktısı 2-B hidrodinamik modelin girdisi, ya da 1-B ve 2-B hidrodinamik modellerin çıktıları 3-B hidrodinamik modelin girdisi olacak şekilde HİDROTÜRK modelinin kullanıcı dostu arayüzü üzerinden yönetilmekte, böylelikle kullanıcıdan kaynaklanabilecek hatalar en az düzeye indirilmektedir.

1-B hidrodinamik model, akış yönünde yazılan yavaş değişen kararsız akış denklemleri olan Saint Venant denklemlerini sayısal olarak çözmekte ve dinamik dalga ötelemesi uygulamaktadır. 1-B boyutlu modellerin kullanımı genişliği az olan uzun nehirlerdeki akışların, bu akışların su yapıları ile etkileşimlerinin ve taşkın olaylarının benzeştirilmesinde önemli araçlardır. 1-B hidrodinamik model olarak, dünyada da yüzey suyu modellemelerinde yaygın olarak kullanılmakta olan açık kaynak kodlu EXTRAN(Extended Transport Model) fortran dili yazılımı düzenlenmiş ve kullanıcı arayüzü üzerinden açık veya kapalı kanallar ve boru sistemlerindeki akışlar için kolaylıkla uygulanabilen bir yapıya getirilmiştir. Modelde, kanal yada boru akış sistemleri, düğüm noktaları ve bunları birleştiren bağlantı hatları ile temsil edilmektedir. Bağlantı hatları akışı düğüm noktalarına iletirler. Akışın debisi bağlantı hatlarındaki temel parametredir. Bağlantı hatlarında momentum denklemi, düğüm noktalarında süreklilik denklemi çözümlenir. Kesitsel akış alanı, su derinliği ve akış hızı her bağlantı hattında değişebilmektedir. 1-B model, arazi üzerinde tanımlanan hesap noktalarından hidrograf verilerini okuyabilmekte ve taşkın akımını ana drenaj hattından dinamik öteleme yöntemiyle tahliye noktalarına kadar taşıyabilmekte; dallanan ve döngüsel ağları, su düzeyi kabarmasını, serbest yüzey akışını, basınçlı akışı veya sürşarjı, ters akışı; savaklar, orifis ve pompa ile akış transferlerini ve açık veya kapalı tesislerdeki depolamanın benzetimini gerçekleştirebilmektedir. Modelde uygulanabilen kanal tipleri dairesel, dikdörtgen, üçgen, trapez veya doğal kesitli kanallar olarak değişmektedir. Kesitler üzerinde köprü ayakları ya da menfezler de tanımlanabilmekte, ve su düzeyi değişimleri için en kesit ve boy kesit profillerinin zamansal değişimleri elde edilebilmektedir. Kanallardaki su derinliği ve su yüzeyi yükseklikleri, deşarj debisi, ve akıntı hızları model çıktıları olarak düzenlenmiştir. Bir yüzeysel su akışı sistemi model ile analiz edilmek istendiğinde, çalışmanın ilk adımı akış sisteminin, havzanın ve alt-havzaların tanımlanmasıdır. Alt-havzaların her biri yüzeyinde oluşan akıntıları, tanımlanan bir drenaj kanalına tahliye eder. Drenaj güzergahlarında kabarma, sürşarj, çevirme-yönlendirme yapıları gibi akım ve su yüksekliği hesabına etki edebilecek yerlerde bir hesap noktası konulması gereklidir. Drenaj güzergahlarında hesap noktası atanması gereken yerler: memba başlangıç noktası, tahliye noktası, pompa istasyonu, depolama alanı, orifis ve savaklar, hidrograf verilerinin tanımlandığı alt-havza giriş noktaları, boru/kanal kesitinin ya da ölçülerinin belirgin şekilde değiştiği noktalar, boru/kanal

eğiminin değiştiği noktalardır. 1-B model hidrodinamik model doğrudan zaman adımlı sayısal bir modeldir.

2-B hidrodinamik model, derinlik boyunca ortalaması alınmış, kararsız süreklilik ve hareket denklemlerini sayısal olarak çözümlemekte olup, yüzey alanı büyüklüğünün su derinliğine göre çok daha baskın olduğu sığ sular için veya su derinliği boyunca tam karışımlı su kütleleri için daha güvenilir benzeşimler sunmaktadır. 2-B modelin sayısal çözümleme yöntemleri, 3-B model ile benzerdir. Modellerin girdileri, rüzgar ve gelgit özellikleri, başlangıç koşulları, yüzey akışı sınır koşulları ve su derinlikleri olup, su düzeyi değişimleri, yoğunluk değişimleri, ve hız değişimleri ise çıktılarıdır. Tüm model girdileri ve çıktıları, kullanıcı dostu arayüz üzerinden yönetilmektedir.

3-B hidrodinamik model, kararsız Navier-Stokes denklemlerini yalnızca Bousinessq varsayımı ile üç boyutta sayısal olarak çözümlemekte, zamanla değişen rüzgar ve yoğunluk gradyanı etkenli akıntıları alansal ve derinlik boyunca benzeştirebilmektedir. Su sıcaklığının, tuzluluğun, basıncın ve yoğunluğun zamansal, alansal ve derinlik boyunca değişimleri incelenebilmektedir. Su kütlesinin derinlikleri fazla olduğunda ve özellikle rüzgar ve yoğunluk kaynaklı çevrintiler gibi su kolonu boyunca yön değiştirebilen akıntıların hesaplanmasında 3-B hidrodinamik modelin kullanılması gereklidir. Geliştirilen iki ve üç boyutlu baroklinik hidrodinamik sayısal modellerde sigma koordinat dönüşümü uygulanmış ve şaşırtmacalı bir çözüm ağı üzerinde dolaylı zaman adımlı sonlu farklar yöntemi kullanılmıştır. Sigma koordinat sitemi, çözüm ağı aralıklarının yüzey ve taban tabakaları arasında sabit olması, her kesitte düşeydeki çözüm noktası sayısının eşit olması ve taban topografyasının düzenli bir biçimde takip edilebilmesi gibi sayısal çözümleme avantajları sağlamaktadır.

Modellerin yazılım geliştirmeleri, bir yüzey suyu yönetim modeli olan SWMM5.0 ve bir kıyı ve geçiş suları yönetim modeli olan üç boyutlu hidrodinamik ve taşınım modeli HYDROTAM-3D ile karşılaştırmalı ön testleri başarıyla tamamlanmıştır. Hidrodinamik modellerin ölçümsel veriler ile doğrulama çalışmaları halen devam etmektedir. Bu makalede hidrodinamik modellerin Gediz Nehri Havzası'nda yer alan Demirköprü Baraj Gölü'ne bazı uygulamaları sunulmuştur. Gelinen bu aşamada, HİDROTÜRK modelinin, bir, iki ve üç boyutlu hidrodinamik alt modellerinin doğrulama çalışmalarına devam edilmesi, bu amaçla eş zamanlı ve uzun süreli olarak hidrodinamik ve kalite parametrelerin Türkiye'nin çeşitli nehir havzalarında ve su kütlelerinde ölçümlenmesi gereklidir.